



Mucoadhesive capsules based on bacterial nanocellulose and chitosan as delivery system of turmeric extract

Laia Posada^a, Natalia Jaramillo-Quiceno^a, Cristina Castro^a, Marlon Osorio^{a,b,*}

^a School of Engineering, Universidad Pontificia Bolivariana, Circular 1°, No. 70-01, Medellín, 050031, Colombia

^b School of Health Science, Grupo de Investigación Biología de Sistemas, Universidad Pontificia Bolivariana, Calle 78B No. 72a-159, Medellín, 050036, Colombia

ARTICLE INFO

Keywords:

Mucoadhesive
Bacterial nanocellulose
Crosslinked chitosan
Turmeric extract
Encapsulation

ABSTRACT

Current efforts in stomach-related drug design focus on improving drug bioavailability within the gastric region. Bacterial nanocellulose (BNC) has been established as a suitable material for drug delivery systems; however, it lacks adhesion to the gastric environment. This limitation can be addressed by leveraging the mucoadhesive properties of low molecular weight chitosan (LMWC). Therefore, we aimed to develop mucoadhesive capsules constructed from BNC coated with crosslinked LMWC, intended for targeted drug delivery in the gastric region. The capsules were characterized using scanning electron microscopy, infrared spectroscopy, thermogravimetric analysis, and mucoadhesion assessments. Under acidic conditions, crosslinked chitosan exhibited enhanced swelling relative to neutral conditions. The coating of chitosan onto the BNC fibrillar network of the capsules resulted in the superimposition of vibration bands and enhanced thermal stability. Furthermore, the capsules exhibited significant mucoadhesive properties in the gastric environment, with an attachment force measuring 89.151 ± 6.226 mN. To validate the efficacy of the system, we utilized antioxidant turmeric extract (TE) as a bioactive compound with chemopreventive potential against stomach cancer. TE was adsorbed onto BNC in a reversible multilayer system, enabling controlled adsorption and desorption. These findings highlight the significance of developing mucoadhesive capsules as a tailored drug delivery system for gastric conditions, particularly in the context of treating stomach diseases as cancer.

1. Introduction

Bacterial nanocellulose (BNC) constitutes a natural polysaccharide composed of linked units of β -1,4-D-(+)-glucose [1]. BNC serves as an efficient drug delivery system for bioactive compounds due to its mechanical attributes, biocompatibility, adsorption capacity, and delivery efficiency [2]. It has also been utilized for encapsulating natural extracts, such as curcumin, to enhance their bioavailability [3,4]. Notably, BNC has received recognition as a safe substance by the USA Food and Drug Administration (FDA) since 1992 and has found applications as a dietary fiber [5,6], food additive, and food substitute, offering benefits such as reduced calorie and fat intake, improved formulation viscosity and stability, and reduced moisture loss from food products [5,6]. Furthermore, it has been employed for immobilizing compounds and facilitating their passage through the gastrointestinal system. However, its application for drug delivery to the stomach has remained limited owing to its lack of mucoadhesive properties with stomach mucus [7–11].

* Corresponding author. School of Engineering, Universidad Pontificia Bolivariana, Circular 1°, No. 70-01, Medellín, 050031, Colombia.
E-mail address: marlonandres.osorio@upb.edu.co (M. Osorio).

<https://doi.org/10.1016/j.heliyon.2023.e21836>

Received 16 May 2023; Received in revised form 27 October 2023; Accepted 30 October 2023

Available online 4 November 2023

2405-8440/© 2023 The Authors. Published by Elsevier Ltd. This is an open access article under the CC BY-NC-ND license (<http://creativecommons.org/licenses/by-nc-nd/4.0/>).

Chitosan, a biopolymer derived from partial deacetylation of chitin, has surfaced as a mucoadhesive [12]. Comprising 2-acetamide-2-deoxy- β -D-glucose and 2-amine-2-deoxy- β -D-glucose units [7,13], chitosan stands out for its biocompatibility, biodegradability, and ability to generate mucoadhesion via its positive surface charge [4,5].

Mucoadhesive systems play a pivotal role in cancer chemoprevention and drug delivery by enhancing the bioavailability of active agents and extending the interaction time between drugs and membranes, thus promoting drug penetration into mucosal layers [7,8]. Moreover, mucoadhesives shield drugs from degradation by gastric acids [8,9]. Chitosan's mucoadhesive properties are subject to control by both physiological and physicochemical factors [5]. For instance, a decrease in chitosan's molecular weight results in stronger adhesion and deeper interpenetration owing to its shorter chain length [6,7]. Additionally, chemical crosslinking reduces the solubility of chitosan under acidic conditions [8]. Various crosslinking methods, such as covalent or ionic bonds using substances like sodium tripolyphosphate (TPP), have been employed, given their safety profile as FDA-approved food and oral drug additives at low concentrations [14–17].

Van der Lubben et al. (2003) harnessed TPP crosslinking via agitation, sonication, and lyophilization to create chitosan microparticles loaded with diphtheria toxoid (DT) for oral and nasal administration. Their findings indicated a significant increase in systemic and local responses following oral administration of DT-loaded chitosan microparticles, yielding dose-dependent systemic immune responses. However, nasal administration yielded no systemic response owing to the lack of mucoadhesiveness of the system in nasal conditions (neutral pH) [18]. Similarly, Xu and Du (2003) developed chitosan nanoparticles via TPP addition to chitosan-containing bovine serum albumin (BSA) under agitation. They observed alterations in the physicochemical structure of chitosan nanoparticles due to enhanced inter- and intramolecular interactions resulting from TPP crosslinking [19]. Additionally, they noted that the fundamental parameters of chitosan, such as molecular weight and degree of deacetylation, influenced the loading and delivery of proteins. For instance, as the degree of deacetylation increased from 75.5 % to 92 % and the molecular mass from 10 kDa to 210 kDa, the encapsulation efficiency increased, whereas the release rate decreased [19].

Turmeric (*Curcuma longa*) extract (TE) represents a natural phytochemical under investigation for its potential in stomach cancer chemoprevention [20]. TE is rich in curcuminoids, with curcumin being the most abundant (IUPAC name 1E,6E-1,7-bis (4-hydroxy-3-methoxyphenyl)-1,6-heptadiene-3,5-dione) [20,21]. has exhibited therapeutic potential in various chronic diseases, including its ability to modulate immunoeediting processes that resurrect immune surveillance mechanisms involved in eradicating cancer cells [22, 23]. However, the low solubility and pharmacokinetic profile of curcumin necessitate high doses for therapeutic efficacy, limiting its clinical relevance [20,21]. Strategies to overcome these limitations, such as encapsulation systems for optimizing bioavailability, have been developed [4,24].

Tsai et al. (2018) proposed curcumin-based mucoadhesive systems using TPP-crosslinked chitosan capsules. Their results show altered alterations in epidermal growth factor (EGF) when the system served as a photosensitizer for photodynamic therapy of gastric cancer cells, particularly those limited to superficial tumors *in vitro* [25]. Similarly, Chuah et al. (2013) explored different concentrations of curcumin using a similar system and observed that the positive electric charge of chitosan's NH_3^+ groups was deprotonated at a neutral/alkaline pH (colon pH), hindering its complete mucoadhesive functionality compared with its performance under acidic conditions [24].

Therefore, we devised a novel technique, wherein we integrated biomaterials (BNC and low molecular weight chitosan [LMWC]) with food-grade natural extracts (TE) to create a mucoadhesive food additive with potential applications in stomach cancer chemoprevention. Furthermore, we comprehensively characterized the chemical, mechanical, morphological, and thermal properties of mucoadhesive capsules, as well as modeled the adsorption and desorption profiles to assess the efficacy of TE delivery. We believe that our findings would hold promise for advancing stomach cancer chemoprevention and improving drug delivery systems.

2. Material and methods

2.1. Materials

Analytical-grade reagents, including LMWC, acetic acid, D-(+)-glucose, potassium dihydrogen phosphate, magnesium sulfate, disodium hydrogen phosphate, citric acid monohydrate, sodium taurocholate, L- α -Phosphatidylcholine, pepsin, sodium chloride, potassium chloride, disodium hydrogen phosphate, and hydrochloric acid, were sourced from Sigma-Aldrich. Bacteriological grade peptone and yeast extracts were acquired from Thermo Fisher Scientific, Inc., whereas food-grade sodium tripolyphosphate (TPP) was obtained from a local distributor. Food-grade turmeric extract (TE) was generously provided by Colorquímica S.A (Colombia).

2.2. Development of bacterial nanocellulose capsules coated with crosslinked LMWC

2.2.1. Development of chitosan mucoadhesive coating

To create a mucoadhesive coating, LMWC and TPP were crosslinked. Three different chitosan concentrations were assessed: 0.67, 1.3, and 2.6 mg/mL. Chitosan was dissolved in a 2 mg/mL acetic acid solution and crosslinked with 0.1 % w/v, following the method by Xu & Du (2003) [19]. The resulting coatings were poured into Petri dishes and air-dried gravimetrically for 24 h (w_0).

Swelling kinetics of the crosslinked chitosan films were measured using a gravimetric method to quantify water adsorption. These experiments were conducted in two different pH solutions (1.6 for the stomach and 7.0 for the colon) using five samples. Films were hydrated with simulated stomach and colon fluid solutions at room temperature (25 °C). Films were periodically removed from the solutions (at 5, 10, 20, 30, 60, and 120 min) and weighed (w_t) [26]. Swelling percentage was calculated using Equation (1).

Table 1

Models employed for describing the adsorption process of the golden latte formulation with 0.1 % CU in BNC pellets. Adapted from Saadi et al. (2015) and Ebadi et al. (2009) [35], [36].

Model	Equation	Parameters
Langmuir	$Q_e = \frac{Q_{ml} K C_e}{1 + K C_e}$	K: Langmuir affinity constant (mL/μg) Q _{mL} : Maximum concentration of adsorbate in the monolayer (μg TE/g BNC)
Freundlich	$Q_e = K_f C_e^{1/n_f}$	k _f : Adsorption coefficient. Represents the adhesion capacity of the adsorbate in the adsorbent 1/n _f : Adsorption intensity of the adsorbate in the adsorbent
BET	$Q_e = \frac{Q_{m,BET} C_{BET} C_e}{(C_e - C_s) \left[1 + (C_{BET} - 1) \frac{C_e}{C_s} \right]}$	Q _{m,BET} : Maximum concentration of adsorbate in the monolayer (μg TE/g BNC) C _{BET} : BET constant C _s : Adsorbate saturation concentration in the monolayer (μg/mL)
BET Modification	$Q_e = Q_m \frac{K_s C_e [1 - (n+1)(K_L C_e)^n + n(K_L C_e)^{n+1}]}{(1 - K_L C_e) \left[1 + \left(\frac{K_s}{K_L} - 1 \right) K_L C_e - \left(\frac{K_s}{K_L} \right) (K_L C_e)^{n+1} \right]}$	Q _{m,BET} : Maximum concentration of adsorbate in the monolayer (μg TE/g BNC) K _s : adsorption equilibrium constant in the monolayer (mL/μg) K _L : adsorption equilibrium constant in the multilayer (mL/μg) n: Maximum number of layers

*C_e: concentration of adsorbate in equilibrium for all models (μg TE/mL).

ω

$$\%S = \frac{w_t - w_0}{w_0} \times 100 \quad (1)$$

Swelling kinetics were determined by plotting the swelling percentage against time, and the simulated fluid solutions for the stomach and colon were prepared following the guidelines of Marques et al. (2011) [27].

2.2.2. Development of bacterial nanocellulose capsules

Bacterial nanocellulose capsules were produced as pellets. The process involved inoculating Hestrin-Schramm (HS)-modified medium with *Komagataeibacter medellinensis* NBRC 3288, with adjustments made to medium volume, agitation speed, and bacterial concentration per volume (detailed in [Supplementary Information 1, S1](#)) following the methodology of Molina-Ramírez et al. (2020) [28]. After 3 d of fermentation under agitation, the pellets were treated with 5 % w/v potassium hydroxide for 14 h and rinsed to reach pH 7 [29,30]. The BNC pellets were then coated using crosslinked LMWC as follows: 1 g of BNC pellets was immersed in a 0.1 % w/v TPP solution for 24 h, after which they were placed in an acetic acid-dissolved chitosan solution (1.3 mg/mL) for 2 h to form the coating.

2.2.3. Characterization techniques

2.2.3.1. Morphological characterization. Before measurement, samples were freeze-dried for 48 h, as described previously. They were then placed on carbon tape, gold-coated using ionic sputtering, and observed using Jeol® JSM equipment at 20 kV [31]. Images were captured at 200–50,000× magnification to evaluate capsule morphology and changes in the presence of simulated stomach or colon fluid.

2.2.3.2. Chemical characterization. Chemical characterization was performed to identify changes in functional groups within the samples of capsules and coatings. A Fourier transform infrared (FTIR) spectrometer (Nicolet 6700, Thermo Scientific, Waltham, MA, USA) equipped with an attenuated total reflectance (ATR) accessory was used. Spectra were recorded from 4000–400 cm⁻¹ wavenumbers with a resolution of 4 cm⁻¹ using a diamond crystal over 64 scans [32].

2.2.3.3. Thermal behavior. Thermal characterization aimed to estimate changes in the decomposition temperature of coated capsules. Thermogravimetric (TGA) and derivative thermogravimetry (DTG) analyses were performed using a Mettler Toledo (TGA/SDTA 851E). Samples of 10 mg were heated from 30 to 800 °C at a rate of 5 °C/min under controlled nitrogen atmosphere (30 mL/min).

2.2.3.4. Mucoadhesion properties analysis. Mucoadhesion experiments were carried out using a TA-XT PLUS texturometer equipped with a 5 N load cell and compression plates (75 mm in diameter). Before testing, the capsules were lyophilized for 48 h (0.020 mbar vacuum pressure) and placed on a plate with double-sided tape (10 × 10 mm). Pig stomach tissues obtained from a local butcher shop (Medellín, Colombia) were washed with distilled water and placed in simulated stomach or colon solution at 25 °C [12,27]. The mucous membranes were isolated after removing the underlying connective tissues. Tissue samples (approximately 20 × 20 mm) were equilibrated at 37.0 ± 0.5 °C for 15 min before being placed on the compression plate holder [12]. The plate containing the capsules was hydrated with simulated stomach or colon solution. The hydrated frame was then moved downwards to contact the tissue with a force of 0.05 N for 60 s, and subsequently moved upwards at a test speed of 0.5 mm/s to record the adhesion forces [12,27].

2.3. Incorporation of TE in the BNC capsules

2.3.1. Adsorption isotherms

To describe the interactions between BNC and TE, experiments were conducted using 0.1 % w/v TE and 0.1 % w/v TPP as antioxidant formulations (see [Supplementary Information 2](#)). One gram of never-dried BNC pellets was mixed with the formulation and water at different weight ratios and stirred at 100 rpm for 24 h at room temperature (25 °C). After 24 h, aliquots of the solutions were obtained, and the equilibrium concentration (C_e) was determined using a UV–visible spectrophotometer at 424 nm (calibration curve R² = 0.999). The adsorbed amount (Q_e) of TE on BNC was calculated using Equation (2) [33,34].

Table 2

Models utilized to characterize the adsorption and release process of TE (adapted from Kajjumba et al., 2019) [37].

Model	Equation	Parameters
Pseudo first-order (PFO)	$Q_t = Q_e(1 - e^{-k_1 t})$	k ₁ : adsorption rate constant (min ⁻¹)
Pseudo second-order (PSO)	$Q_t = \frac{k_2 Q_e^2 t}{1 + k_2 Q_e t}$	k ₂ : adsorption rate constant (g BNC μg TE ⁻¹ min ⁻¹)
Elovich	$Q_t = \frac{1}{\beta} \ln(\alpha\beta) + \frac{1}{\beta} \ln(t)$	α: Initial adsorption rate (μg/g.min) β: degree of surface coverage (g/μg)
Intraparticle diffusion (IP)	$Q_t = k_3 \sqrt{t}$	k ₃ : adsorption rate constant (μg/g.min ^{0.5})

*Q_t: the amount of TE adsorbed or released in time for all models (μg/g.min).

**Q_e: the amount of TE adsorbed or released at equilibrium for all models (μg/g).

***t: Time for all models (min).

$$Q_e = \frac{C_i - C_e}{W_{BNC}} \times V_T, \quad (2)$$

where C_i is the initial concentration of the antioxidant formulation, V_T is the total volume of the evaluated solution, and W_{BNC} is the evaluated weight of the pellets in grams. Mathematical models used to describe the phenomenon are listed in Table 1, and experimental data were fitted to the models using the least squared method and Solver® tools in Microsoft Excel [35,36].

2.3.2. Adsorption kinetics

Adsorption kinetics were analyzed to determine equilibrium time and understand the adsorption phenomenon in the BNC pellets. Different models were applied, as listed in Table 2 [37]. Experiments were conducted in 50 mL falcon tubes, mixing the formulation with 0.1 % w/v TE with BNC pellets at a ratio of 5:1. Agitation was set at 100 rpm at room temperature (25 °C). Adsorption kinetics were determined by taking 1 mL aliquots of the solution at 5, 10, 20, 30, 60, 120, and 240 min. The equilibrium concentration (C_e) and the amount adsorbed in the BNC pellets over time (Q_t) were calculated, similar to the adsorption isotherms. Experimental data were fitted to the models using the least squared method and Solver® tools in Microsoft Excel [35,36].

2.3.3. Release kinetics

The release profile of the final system, TE loaded into chitosan-coated BNC mucoadhesive capsules, was evaluated using desorption assays. Experiments were conducted in 50 mL falcon tubes by adding 25 mg of loaded capsules per mL of simulated stomach (pH 1.6) or colon (pH 7.0) fluid at 37 °C. Aliquots of 1 mL were taken at 5, 10, 20, 30, 60, 120, 240, 360, 480, and 1440 min. The equilibrium concentration (C_e) and the amount adsorbed in time (Q_t) for each aliquot were determined using the same UV-Vis protocol employed for the adsorption isotherms and were modeled using the equations presented in Table 2.

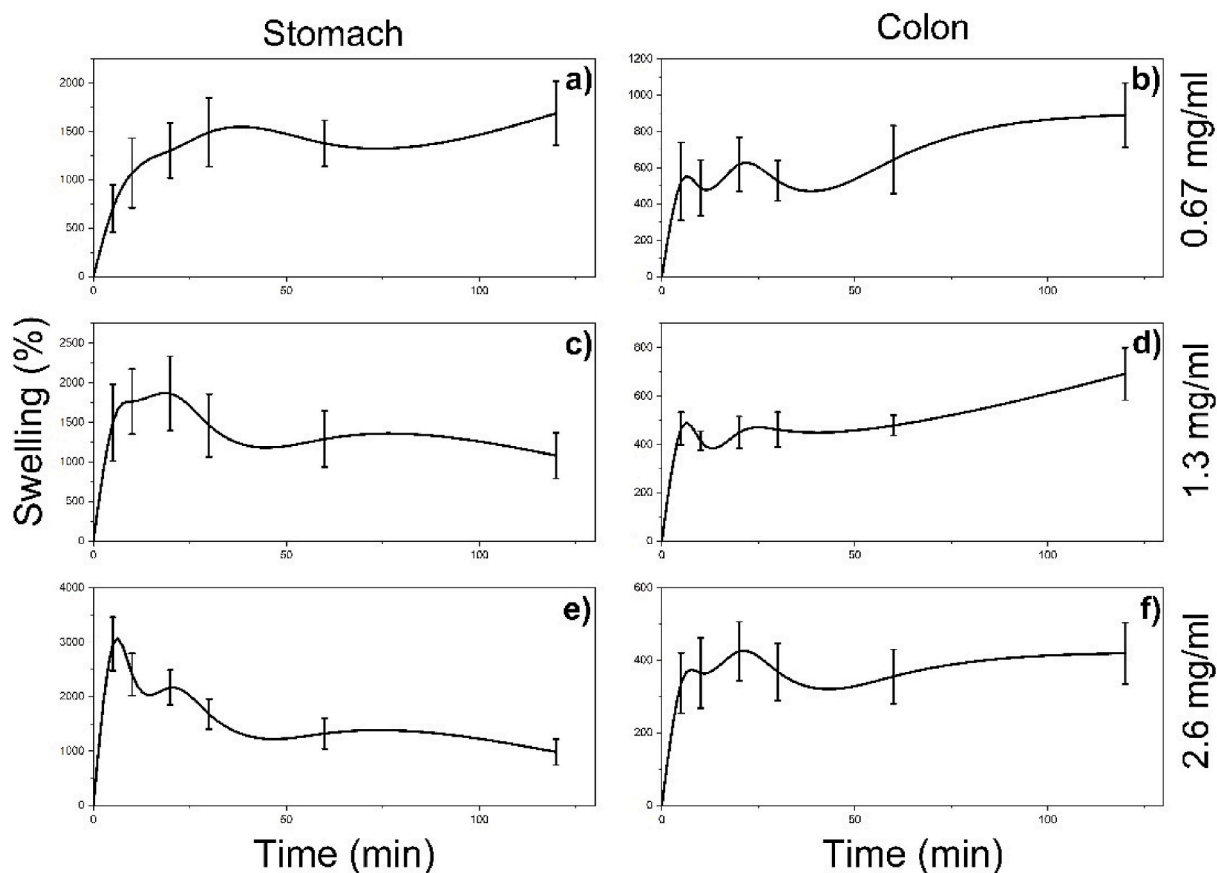


Fig. 1. Swelling kinetics of the crosslinked low molecular weight chitosan (LMWC) with a concentration of 0.67 mg/mL evaluated in a) stomach (pH 1.6) and b) colon (pH 7.0) simulated fluid, 1.3 mg/mL evaluated in c) stomach (pH 1.6) and d) colon (pH 7.0) simulated fluid, and 2.6 mg/mL evaluated in e) stomach (pH 1.6), and f) colon (pH 7.0) simulated fluid.

3. Results and discussion

3.1. Development of bacterial nanocellulose capsules coated with crosslinked LMWC

3.1.1. Development of chitosan-based mucoadhesive

Fig. 1 displays the swelling kinetics of the crosslinked LMWC films in simulated colon and stomach fluids. The films exhibited maximum swelling at different time points, contingent upon the chitosan concentration. After reaching maximum swelling, the capacity gradually diminished until equilibrium was attained, mirroring the behavior documented by Orozco-Guareño et al. (2011) [38]. Our experiments indicated that a chitosan concentration of 1.3 mg/mL (Fig. 1c) demonstrated superior performance in terms of maximum swelling and temporal progress. It reached equilibrium at 20 min with a swelling capacity of 1866 % in the stomach environment, where mucoadhesion is desired. Higher concentrations of chitosan (>1.3 mg/mL) resulted in reduced swelling capacity owing to enhanced molecular interactions between the films, leading to a more closely connected network with reduced structural capacity for swelling (chain movement) [38]. Conversely, lower crosslinking concentrations (<1.3 mg/mL) led to reduced swelling capacity owing to the absence of an interconnected hydrogel network responsible for water adsorption [38].

Regarding pH, LMWC films exhibited higher swelling capacity in acidic pH (see Fig. 1a, c, and 1e) than that at for neutral pH (see Fig. 1b, d, and 1f), indicating selectivity toward the stomach. This highlights that crosslinked LMWC films possess mucoadhesive properties [39,40]. Considering equilibrium time, concentration, and pH selectivity, we selected an LMWC concentration of 1.3 mg/mL for further coating experiments.

3.1.2. Development of bacterial nanocellulose capsules

Based on statistical analysis of fermentation parameters using 160 rpm, 150 mL, and three cryo-pearls, we achieved the highest yield in the process, amounting to 45.03 ± 0.45 g of pellets/L of HS-modified medium (see fermentation parameters in S.1). During this process, the pellets acquired a spherical shape (Fig. 2a). Furthermore, we investigated the impact of coating, as illustrated in Fig. 2b for non-coated capsules and Fig. 2c for coated capsules. In both cases, the capsules exhibited spherical-shaped particles with diameters of 1.05 ± 0.42 mm, a sphericity of 0.63 ± 0.17 (resulting from the tendency of the bacteria to adopt this morphology under agitated conditions), and a translucent color. Notably, after capsule coating, we observed no observable macroscopic changes in diameter, sphericity, or color.

3.1.3. Morphological characterization

Scanning electron microscopy (SEM) images of the samples are presented in Fig. 3a–d. Fig. 3a shows non-coated BNC capsules, whereas Fig. 3b displays BNC capsules coated with mucoadhesive based on crosslinked LMWC. In the case of non-coated capsules, the open fibrillar structure of the BNC was evident. However, when coated with crosslinked LMWC, the fibrillar network appeared closed. Nevertheless, the fibrillar texture remained on the capsule surface.

Fig. 3c and d depict the BNC capsules after 24 h in the stomach and colon, respectively. In both cases, the capsules exhibited a swollen morphology with some surface porosity, more pronounced in the stomach environment where the fibrillar structure of the BNC had completely disappeared. This indicates the selectivity of the system for gastric applications.

3.1.4. Chemical characterization

Fig. 4 displays the FTIR spectra. For the LMWC coating (Fig. 4a), most vibrations occurred in two regions ($3700\text{--}2800\text{ cm}^{-1}$ and $1700\text{--}400\text{ cm}^{-1}$). These results align with previous reports on chitosan in the literature [41]. In the case of the non-crosslinked capsule (Fig. 4b), new bands appeared at wavenumbers of 898 cm^{-1} (indicating the presence of β -1,4 glycosidic glucose bonds) and 1061 cm^{-1} (attributed to glucose glucopyranose ring stretch vibration), representative of BNC. Additionally, for the full system in Fig. 4c (BNC coated with crosslinked LMWC and TPP), vibration intensities increased in the regions $900\text{--}800\text{ cm}^{-1}$ and $1700\text{--}1300\text{ cm}^{-1}$, corresponding to P–O–P and P=O bonds, respectively [39,41,42]. Accordingly, Fig. 4c demonstrates the presence of a crosslinked chitosan coating on the surface of BNC.

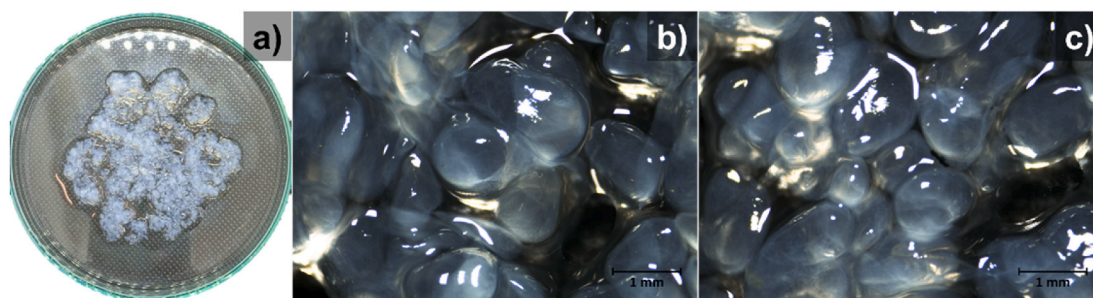


Fig. 2. Bacterial nanocellulose (BNC) capsules: a) Macroscopic view (Petri dish diameter of 10 cm), b) Observation under a stereomicroscope, and c) Capsules coated with crosslinked LMWC. The scale bar represents 1 mm.

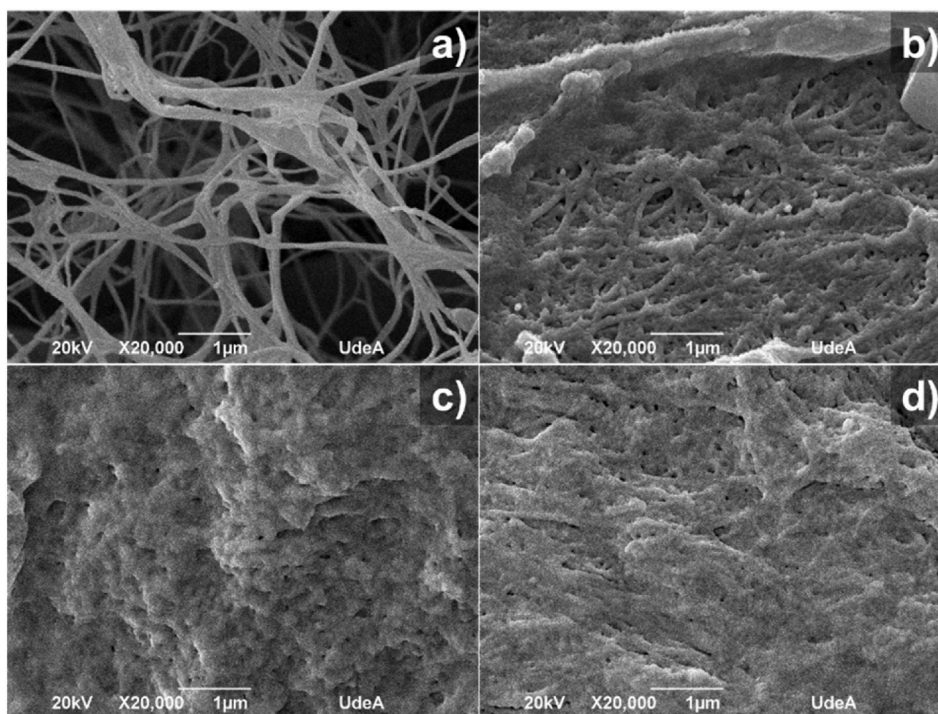


Fig. 3. Scanning electron microscopy (SEM) images: a) BNC capsules, b) BNC capsules coated with crosslinked LMWC (BNC-LMWC-TPP). Images of BNC-LMWC-TPP in simulated c) stomach fluid (pH 1.6) and d) colon fluid (pH 7.0). Images taken at 20,000 × magnification.

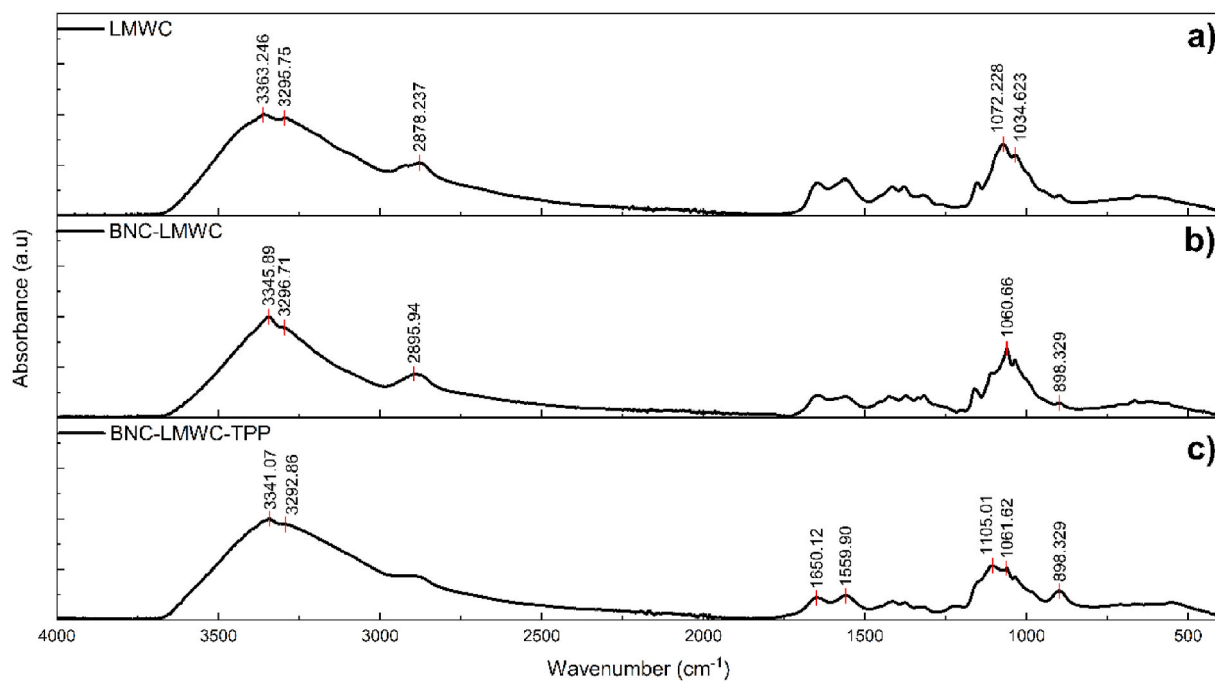


Fig. 4. Chemical characterization of the capsules: Infrared spectra of a) LMWC, b) LMWC with BNC, and c) BNC capsules coated with crosslinked LMWC, with important peaks indicated.

3.1.5. Thermal characterization

The TGA and DTG results are presented in Fig. 5. These results reveal a broad peak in the temperature range between 40 and 150 °C, with the maximum rate occurring at 66 °C for all materials. This peak is attributed to the release of physisorbed water [43]. The

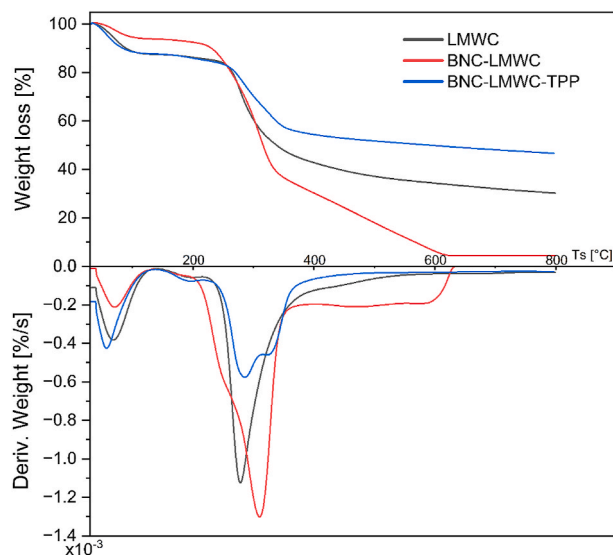


Fig. 5. Thermogravimetric analysis (TGA) curves (top) and derivative thermogravimetry (DTG) (bottom) of LMWC and LMWC mixed with BNC or BNC capsules with crosslinked LMWC and TPP. Degradation peaks of BNC-LMWC-TPP are indicated with arrows.

degradation temperature of chitosan was approximately 280 °C, with a maximum decomposition rate of 1.2×10^{-3} %/min. BNC exhibited its maximum degradation temperature at 300 °C [42].

For the full system (BNC-LMWC-TPP, indicated by the blue line), two maximum degradation peaks were observed: the first at 285 °C and the second at 325 °C. The first corresponds to the interactions between LMWC and TPP (primary bonds), and the second corresponds to the interactions between crosslinked LMWC and BNC. In this case, BNC enhances the thermal stability of LMWC owing to intermolecular hydrogen interactions (secondary bonds) [28]. In terms of decomposition rate, the full system displayed a shift to a higher temperature by 36 °C, indicating the formation of a crosslinked structure. Furthermore, the ash content increased in the presence of phosphorus in the material structure [43].

3.1.6. Mucoadhesion properties

The maximum detachment force (F_{\max}) and adhesion work (W_{ad}) of the capsules (BNC and BNC coated with crosslinked LMWC) when exposed to gastric tissue at different pH values are presented in Fig. 6a and b. In Fig. 6a, BNC capsules under gastric or colonic conditions exhibited an F_{\max} and W_{ad} below 30 mN and 16 mN-mm, respectively, indicating no mucoadhesive properties for BNC capsules, consistent with literature reports [10,11]. However, the coated capsules (BNC-LMWC-TPP) under stomach conditions exhibited $F_{\max} = 89.15 \pm 6.23$ mN and $W_{\text{ad}} = 43.18 \pm 2.85$ mN-mm, whereas under colon conditions, they exhibited $F_{\max} = 37.18 \pm 7.49$ mN and $W_{\text{ad}} = 32.15 \pm 1.56$ mN-mm. This demonstrates that the crosslinked LMWC coating significantly enhances the performance of BNC capsules in both fluids. Notably, the most pronounced results were observed in the stomach environment. For instance, the samples exhibited a 140 % increase in F_{\max} and a 34 % increase in W_{ad} . The behavior of the coated capsules indicates a

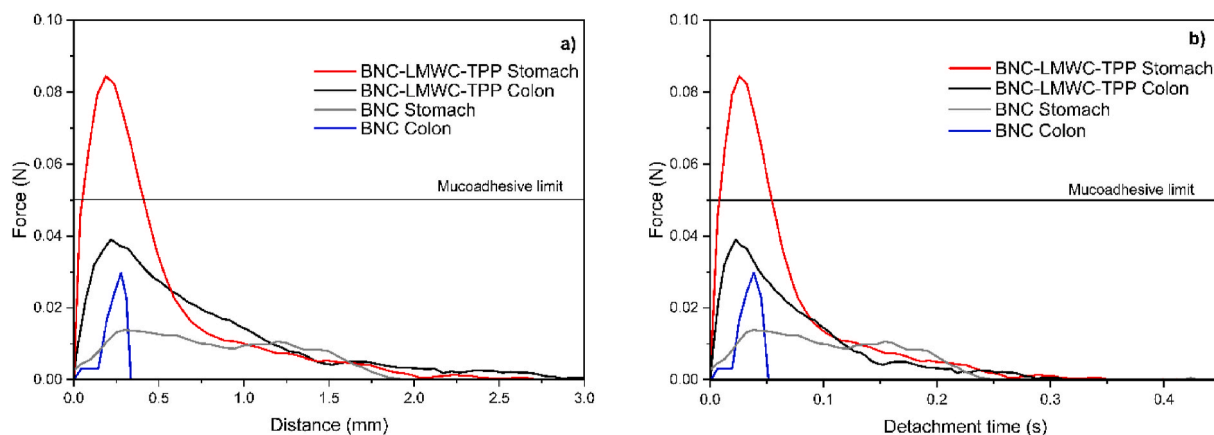


Fig. 6. Mucoadhesion properties of non-coated and LMWC-TPP coated capsules: Force vs a) distance and b) detachment time for capsules of BNC and BNC coated with crosslinked LMWC (BNC-LMWC-TPP) during mucoadhesive testing using a texturometer.

mucoadhesive system (with a lower limit of mucoadhesion at 50 mN [12]), and according to the results, this mucoadhesive performance is selective for stomach conditions, validating the significance of the system for gastric drug delivery.

Detachment times of the capsules, as presented in Fig. 6b, were 25 % faster under colonic conditions (0.32 s) relative to stomach conditions (0.43 s). These findings, in conjunction with the swelling kinetics and SEM results, suggest that the mucoadhesive response of the developed capsules is influenced by pH conditions. The capsules adhere to the stomach mucus via strong electrostatic interactions induced by crosslinked chitosan under acidic conditions [12,26]. Hydrophilically charged polymers such as chitosan form electrostatic interactions through hydrogen bonding and ionic interactions, resulting in high mucoadhesion [10,11]. Furthermore, TPP crosslinking enhances the surface charge of chitosan, creating additional opportunities for stronger secondary interactions that enhance mucoadhesion [25]. BNC alone exhibits insufficient mucoadhesion, measuring below 50 mN under stomach and colon conditions. However, the coating significantly improves mucoadhesion, increasing it by approximately 5.8-fold, from 15 mN to 89 mN. This enhancement in mucoadhesive properties in BNC coated with LMWC-TPP capsules can be attributed to their interaction forces and pH selectivity. These properties are crucial for enhancing the bioavailability of TE in the context of stomach-related conditions, such as cancer.

3.2. Incorporation of TE in the BNC capsules

3.2.1. Adsorption isotherms

The adsorption isotherms of TE in the BNC capsules are presented in Fig. 7 and Table 3. The antioxidant formulation of BNC resembles an L3-type isotherm, typically observed when adsorbed molecules maximize their contact area with the material or when molecules face limited solvent competition, aligning with the modified BET model ($R^2 = 0.987$) [44]. This model comprises a multilayered structure with 24–38 layers, featuring a Q_m of 84.64 μg of TE/g of BNC. This value suggests that the BNC pellets are highly saturated with the formulation, especially when considering the monolayer saturation concentration ($1/K_s$) of 2.38 μg of TE/mL.

3.2.2. Adsorption kinetics

To study adsorption kinetics, a concentration (C_e) of 31.15 μg of TE per mL was utilized to maximize antioxidant capacity, crucial for its chemopreventive therapeutic effect in stomach cancer (see S.2). The adsorption kinetics results are depicted in Fig. 8 and Table 4. The pseudo first-order (PFO) model best fits the kinetics with an R^2 value of 0.889. This model yields a Q_e of 31.52 μg of TE/g of BNC and an adsorption rate (k_2) constant of 0.53 min^{-1} , indicating that the adsorption of the TE formulation onto the adsorbent follows a first-order mechanism, signifying its reversibility [37]. This mechanism is advantageous for BNC capsules as it suggests that the system can deliver TE to the target area, functioning as a delivery system. The capsule reached equilibrium within 20 min, indicative of a rapid adsorption process, favorable for the production of mucoadhesive capsules for TE delivery.

3.2.3. Release profiles

Finally, Fig. 9 a and b, and Table 5 present the release profiles of TE encapsulated in BNC-LMWC-TPP. The most suitable model for fitting depends on the pH. In the case of the stomach (pH 1.6), the PFO model provides the best fit, whereas for the colon (pH 7.0), the experimental data align better with the pseudo second-order (PSO) model.

The release profile under simulated colon fluid at pH 7.0 indicates equilibrium at 60 min, whereas under stomach conditions (pH 1.6), equilibrium is reached at 10 min. The release rate is slower in the colon relative to gastric conditions (see rate constants K_1 and K_2 in Table 5), demonstrating the selectivity of the crosslinked chitosan-based mucoadhesive coating at acidic pH. This enables TE interaction as a bioactive compound with the stomach walls, where gastric cancer may develop, and TE can exert therapeutic effects through its antioxidant mechanism [22]. The TE-releasing performance and mucoadhesive properties of the capsules enhance the bioavailability of TE in the gastric area, facilitating its chemopreventive effects. The mucoadhesive properties of the formulation containing TE enable a specific interaction with the target area, enhancing the antioxidant effects of TE. The TE used in this study exhibited a total polyphenol content of 399.47 ± 27.98 μg of gallic acid/mL and an antioxidant capacity of 1071.83 μg Trolox/mL (see S.2). TE plays a crucial role in modulating immunoediting processes and expression signals necessary for tumor cell proliferation [45, 46]. Additionally, it induces apoptosis in tumor cells through exogenous mechanisms. This mechanism involves reducing the mitochondrial transmembrane potential, leading to an accumulation of reactive oxygen species within the tumor cells. Furthermore, the antioxidant capacity of TE can stimulate immune cells to aid in the eradication of cancer cells [45,46]. Owing to the TE release performance and mucoadhesive properties of the capsules, they contribute to the improved bioavailability of TE in the gastric region. This, in turn, facilitates the chemopreventive effects of TE through the antioxidant mechanism described above.

Stomach release systems that improve TE bioavailability have been reported previously [24,47,48]. These studies demonstrated the chemopreventive effects of TE encapsulation, resulting in a 65 % reduction in stomach cancer cell bioavailability, along with dual mucoadhesive properties, with stronger adhesion observed in stomach tissue compared to the colon [24,47,48], aligning with the findings of this study (a 5.8-fold improvement in mucoadhesion). Consequently, the capsules developed in this study have potential applications in the chemoprevention of stomach cancer. Notably, this technology is safe owing to the mucoadhesion of crosslinked LMWC via secondary interactions, which are not expected to cause irritation, inflammation, or ulceration of the gastric mucosa [10, 11]. Additionally, with an adhesion force of 89 mN under normal stomach conditions and shear stresses (peristaltic movement), the capsules can be readily detached [49]. Other studies have demonstrated that chitosan crosslinked with TPP can adhere to stomach conditions for up to 90 h and is easily cleared from the digestive tract [10,49,50]. Moreover, all components of the system are food-grade and FDA-approved for use in food formulations [17,51].

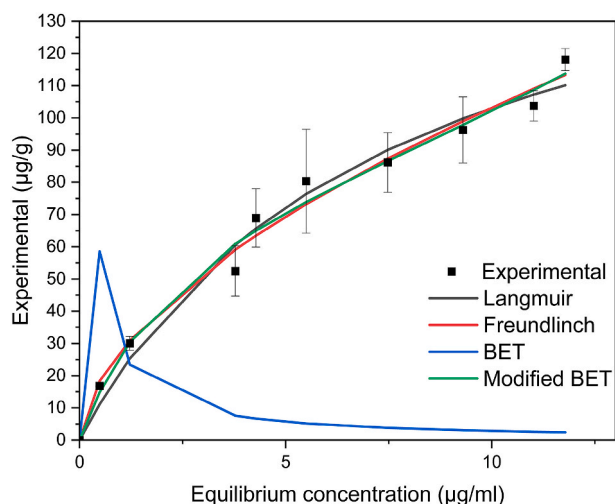


Fig. 7. Adsorption isotherm model fitted to experimental isotherm data of a formulation with 0.1 % w/v TE and 0.1 % w/v TPP on BNC.

Table 3

Models employed for describing adsorption isotherms, along with their corresponding parameters (optimal model adjustments highlighted in red).

Model	Parameters	25 °C	R ²
Monolayer			
Langmuir	K (mL/µg)	0.135	0.982
	Q _{mL} (µg TE/g BNC)	179.36	
Freundlich	k _f	27.62	0.986
	n _f	1.75	
Multilayer			
BET	Q _m , BET (µg TE/g BNC)	7337221.28	-2.765
	CBET	2885.76	
	C _s (µg/mL)	0.00	
Modified BET	Q _{m,BET} (µg TE/g BNC)	84.64*	0.987*
	K _S (mL/µg)	0.42*	
	K _L (mL/µg)	0.03*	
	n	24.38*	

*Best modeling fitness.

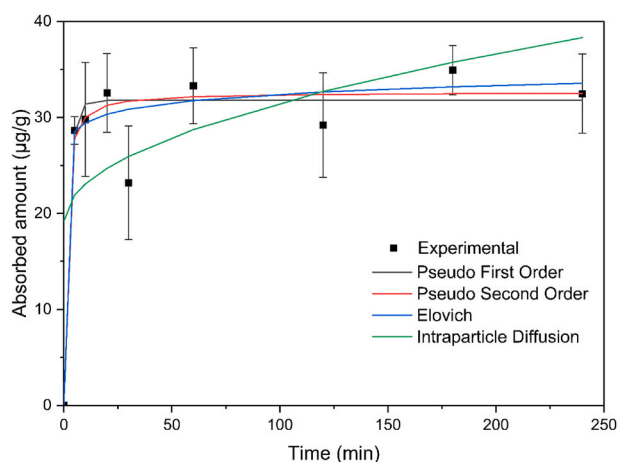


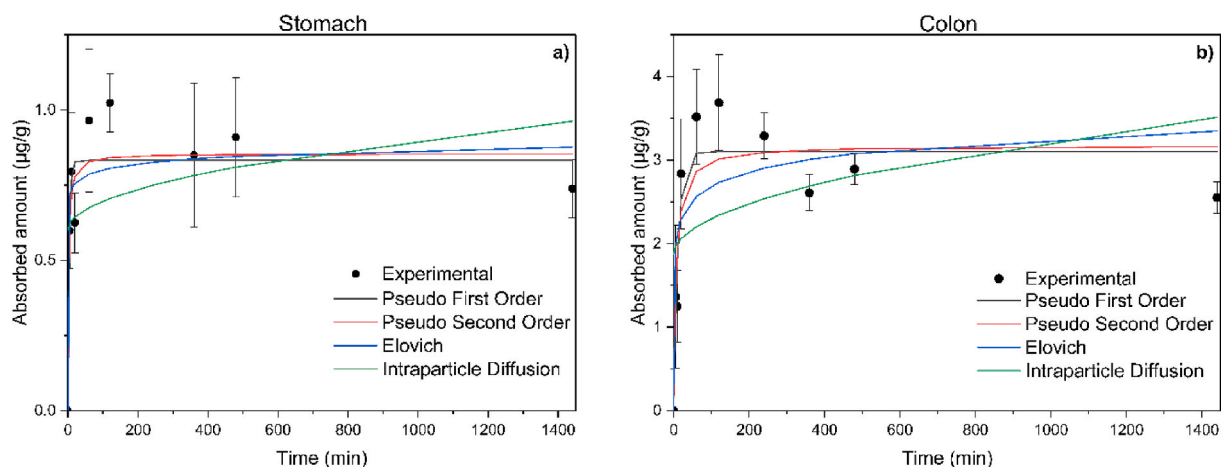
Fig. 8. Adsorption kinetic models fitted to experimental data.

Table 4

Models utilized for describing the adsorption kinetics of the formulation containing 0.1 % w/v TE and 0.1 % w/v TPP on BNC.

Model	Parameter	25 °C	R ²
PFO	Q _e (μg TE/g BNC)	31.52*	0.889*
	k ₁ (min ⁻¹)	0.53*	
PSO	Q _e (μg TE/g BNC)	31.61	0.885
	k ₂ (g BNC μg TE ⁻¹ min ⁻¹)	0.13	
Elovich	α (μg TE/g BNC·min)	2.42 × 10 ²³	0.887
	B (g BNC/μg TE)	1.87	
IP	C (μg TE/g BNC)	19.92	0.287
	K ₃ (μg TE/g BNC·min ^{0.5})	1.12	

*Best modeling fitness.

**Fig. 9.** Release profiles of TE from mucoadhesive capsules BNC-LMWC-TPP in simulated a) stomach conditions and b) colon conditions.**Table 5**

Profiles of TE release from BNC-LMWC-TPP capsules in simulated conditions, along with their respective parameters.

Model	Parameter	TE-BNC with LMWC	
		pH 1.6	pH 7.0
PFO	Q _e (μg TE/g BNC)	0.83	3.10*
	k ₁ (min ⁻¹)	0.25	0.09*
	R ²	0.823	0.870*
PSO	Q _e (μg TE/g BNC)	0.86*	3.18
	k ₂ (min ⁻¹)	0.61*	0.05
	R ²	0.832*	0.817
Elovich	α (μg TE/g BNC·min)	5.76 × 10 ⁸	133.52
	B (g BNC/μg TE)	35.37	4.052
	R ²	0.791	0.661
IP	C (μg TE/g BNC)	0.60	1.87
	K ₃ (μg TE/g BNC·min ^{0.5})	0.01	0.04
	R ²	0.147	0.186

*Best modeling fitness.

4. Conclusions

We have successfully developed a mucoadhesive system based on BNC coated with TPP-crosslinked LMWC as a delivery system for TE in the stomach. The swelling of the LMWC coating was influenced by chitosan concentration, with 1.3 mg of LMWC/mL exhibiting superior swelling and mucoadhesion. Furthermore, mucoadhesion of BNC capsules coated with crosslinked LMWC was selective under acidic pH conditions (gastric conditions). Chemical characterization confirmed the crosslinking reaction and interaction between BNC and LMWC. Adsorption of TE resulted in the formation of a stable, reversible, and homogeneous multilayer on the BNC surface. The system achieved equilibrium within 20 min, indicating a short adsorption process conducive to the production of mucoadhesive capsules for TE delivery.

Collectively, our findings demonstrate the potential of these capsules to enhance TE presence in stomach tissue, rendering it a

promising strategy for chemoprevention of stomach cancer. Notably, this technology is safe, and all components are FDA-approved for use in food formulations. Future research should focus on evaluating long-term stability, safety, and conducting animal studies to understand the behavior of these capsules in complex systems.

Funding

This study was supported by the *Ministerio de Ciencia Tecnología e Innovación* (Minciencias) Project Nanovehículos 92355 of the Program 92332 “*Avance en el desarrollo de alternativas preventivas y terapéuticas basadas en nanobioconjugados para el tratamiento del cáncer colorrectal en Colombia* (NanoBioCancer 2.0 GAT 2.0. Cod. 121092092332, Contract number: 621–2022), by Minciencias, Mineducación, Mincit, and ICETEX, through the Program Ecosistema Científico Cod. FP44842-211-2018, project number 58674, and by the project APSC874-2020 Cod. M801PR15F05.

Data availability statement

Data included in article/suppl. Material/referenced in article.

CRediT authorship contribution statement

Laia Posada: Formal analysis, Investigation, Writing – original draft, Writing – review & editing, Funding acquisition. **Natalia Jaramillo-Quiceno:** Data curation, Writing – review & editing. **Cristina Castro:** Conceptualization, Funding acquisition, Methodology, Project administration, Writing – review & editing. **Marlon Osorio:** Conceptualization, Data curation, Formal analysis, Investigation, Methodology, Supervision, Writing – review & editing.

Declaration of competing interest

The authors declare that they have no known competing financial interests or personal relationships that could have appeared to influence the work reported in this paper.

Acknowledgements

The authors thank Colorquímica S.A. Colombia for kindly donating food-grade turmeric extract. The authors thank Mr. Juan Lara Patiño for technical assistance with the LMWC swelling experiments.

Appendix A. Supplementary data

Supplementary data to this article can be found online at <https://doi.org/10.1016/j.heliyon.2023.e21836>.

References

- [1] M. Osorio, A. Cañas, J. Puerta, L. Díaz, T. Naranjo, I. Ortiz, et al., Ex vivo and in vivo biocompatibility assessment (blood and tissue) of three-dimensional bacterial nanocellulose biomaterials for soft tissue implants, *Sci. Rep.* 9 (2019) 10553, <https://doi.org/10.1038/s41598-019-46918-x>.
- [2] M. Osorio, et al., Lignocellulosic materials for biomedical applications, in: *Lignocellulosics: Renewable Feedstock for (Tailored) Functional Materials and Nanotechnology*, Elsevier, 2020, pp. 209–248, <https://doi.org/10.1016/B978-0-12-804077-5.00013-0>.
- [3] A. Gupta, D.J. Keddie, V. Kannappan, H. Gibson, I.R. Khalil, M. Kowalczyk, et al., Production and characterisation of bacterial cellulose hydrogels loaded with curcumin encapsulated in cyclodextrins as wound dressings, *Eur. Polym. J.* 118 (2019) 437–450, <https://doi.org/10.1016/j.eurpolymj.2019.06.018>.
- [4] M. Zikmundova, M. Vereshaka, K. Kolarova, J. Pajorova, V. Svorcik, L. Bacakova, Effects of bacterial nanocellulose loaded with curcumin and its degradation products on human dermal fibroblasts, *Materials* 13 (2020) 1–17, <https://doi.org/10.3390/ma13214759>.
- [5] Q. Lu, X. Yu, A.E.A. Yagoub, H. Wahia, C. Zhou, Application and challenge of nanocellulose in the food industry, *Food Biosci.* 43 (2021), 101285.
- [6] H.M.C. Azeredo, H. Barud, C.S. Farinas, V.M. Vasconcellos, A.M. Claro, Bacterial cellulose as a raw material for food and food packaging applications, *Front. Sustain. Food Syst.* 3 (2019), <https://doi.org/10.3389/fsufs.2019.00007>.
- [7] R. Harris, N. Acosta, A. Heras, Chitosan and Inhalers: A Bioadhesive Polymer for Pulmonary Drug Delivery, Elsevier Masson SAS, 2013, <https://doi.org/10.1533/9780857098696.2.77>.
- [8] R. Shaikh, T.R. Raj Singh, M.J. Garland, A.D. Woolfson, R.F. Donnelly, Mucoadhesive drug delivery systems, *J. Pharm. BioAllied Sci.* 3 (2011) 89–100, <https://doi.org/10.4103/0975-7406.76478>.
- [9] N.A.N. Hanafy, S. Leporatti, M.A. El-Kemary, Mucoadhesive hydrogel nanoparticles as smart biomedical drug delivery system, *Appl. Sci.* 9 (2019) 825, <https://doi.org/10.3390/app9050825>.
- [10] J. Singh, N.C.S. Tan, U.R. Mahadevaswamy, N. Chanchareonsook, T.W.J. Steele, S. Lim, Bacterial cellulose adhesive composites for oral cavity applications, *Carbohydr. Polym.* 274 (2021), 118403, <https://doi.org/10.1016/j.carbpol.2021.118403>.
- [11] N. Ahmad, M.C.I.M. Amin, S.M. Mahali, I. Ismail, V.T.G. Chuang, Biocompatible and mucoadhesive Bacterial cellulose-g-poly(acrylic acid) hydrogels for Oral Protein Delivery, *Mol Pharm.* Nov. 11 (2014) 4130–4142, <https://doi.org/10.1021/mp5003015>.
- [12] N. Thirawong, J. Nunthanid, S. Puttipatkhachorn, P. Sriamornsak, Mucoadhesive properties of various pectins on gastrointestinal mucosa: an in vitro evaluation using texture analyzer, *Eur. J. Pharm. Biopharm.* 67 (2007) 132–140.
- [13] L. Urbina, O. Guaresti, J. Requies, N. Gabilondo, A. Eceiza, M.A. Corcuera, et al., Design of reusable novel membranes based on bacterial cellulose and chitosan for the filtration of copper in wastewaters, *Carbohydr. Polym.* 193 (2018) 362–372, <https://doi.org/10.1016/j.carbpol.2018.04.007>.

- [14] M.C. Gómez-Guillén, M.P. Montero, Enhancement of oral bioavailability of natural compounds and probiotics by mucoadhesive tailored biopolymer-based nanoparticles: a review, *Food Hydrocolloids* 118 (2021), 106772, <https://doi.org/10.1016/j.foodhyd.2021.106772>.
- [15] A. Subramanian, H.Y. Lin, Crosslinked chitosan: its physical properties and the effects of matrix stiffness on chondrocyte cell morphology and proliferation, *J Biomed Mater Res A*. Dec. 75 (2005) 742–753, <https://doi.org/10.1002/jbm.a.30489>.
- [16] C. Ryan, E. Alcock, F. Buttner, M. Schmidt, D. Clarke, M. Pemble, et al., Synthesis and characterisation of cross-linked chitosan composites functionalised with silver and gold nanoparticles for antimicrobial applications, *Sci. Technol. Adv. Mater.* 18 (2017) 528–540, <https://doi.org/10.1080/14686996.2017.1344929>.
- [17] FDA, U.S Food & Drug Administration. CFR – code of federal regulations Title 21. [Cited Oct. 05, 2021]. Available from: <https://www.accessdata.fda.gov/scripts/cdrh/cfdocs/cfCFR/CFRSearch.cfm?fr=182.1810>; 2021..
- [18] I.M. van der Lubben, G. Kersten, M.M. Fretz, C. Beuvery, J.C. Coos Verhoef, H.E. Junginger, Chitosan microparticles for mucosal vaccination against diphtheria: oral and nasal efficacy studies in mice, *Vaccine* 21 (2003) 1400–1408, [https://doi.org/10.1016/S0264-410X\(02\)00686-2](https://doi.org/10.1016/S0264-410X(02)00686-2).
- [19] Y. Xu, Y. Du, Effect of molecular structure of chitosan on protein delivery properties of chitosan nanoparticles, *Int. J. Pharm.* 250 (2003) 215–226, [https://doi.org/10.1016/S0378-5173\(02\)00548-3](https://doi.org/10.1016/S0378-5173(02)00548-3).
- [20] E. Willenbacher, S.Z. Khan, S.C.A. Mujica, D. Trapani, S. Hussain, D. Wolf, et al., Curcumin: new insights into an ancient ingredient against cancer, *Int. J. Mol. Sci.* 20 (2019) 1–13, <https://doi.org/10.3390/ijms20081808>.
- [21] A. Giordano, G. Tommonaro, Curcumin and cancer, *Nutrients* 11 (2019) 2376, <https://doi.org/10.3390/nu11102376>.
- [22] A. Thyagarajan, R.P. Sahu, Potential contributions of antioxidants to cancer therapy: immunomodulation and radiosensitization, *Integr. Cancer Ther.* 17 (2018) 210–216, <https://doi.org/10.1177/1534735416681639>.
- [23] M. Dei Cas, R. Ghidoni, Dietary curcumin: correlation between bioavailability and health potential, *Nutrients* 11 (2019) 1–14, <https://doi.org/10.3390/nu11092147>.
- [24] L.H. Chuah, N. Billa, C.J. Roberts, J.C. Burley, S. Manickam, Curcumin-containing chitosan nanoparticles as a potential mucoadhesive delivery system to the colon, *Pharmaceut. Dev. Technol.* 18 (2013) 591–599, <https://doi.org/10.3109/10837450.2011.640688>.
- [25] W.H. Tsai, K.H. Yu, Y.C. Huang, C.I. Lee, EGFR-targeted photodynamic therapy by curcumin-encapsulated chitosan/TPP nanoparticles, *Int. J. Nanomed.* 13 (2018) 903–916, <https://doi.org/10.2147/IJN.S148305>.
- [26] E. Orozco-Guareño, S. Hernández, S. Gómez-Salazar, E. Mendizábal, I. Katime, Estudio del hinchamiento de hidrogeles acrílicos terpoliméricos en agua y en soluciones acuosas de ión plumboso, *Rev. Mex. Ing. Quim.* (2011) 465–470.
- [27] M.R.C. Marques, R. Loebenberg, M. Almukainzi, Simulated biological fluids with possible application in dissolution testing, *Dissolution Technol.* 18 (2011) 15–28, <https://doi.org/10.14227/DT180311P15>.
- [28] C. Molina-Ramírez, A. Cañas-Gutiérrez, C. Castro, R. Zuluaga, P. Gañán, Effect of production process scale-up on the characteristics and properties of bacterial nanocellulose obtained from overripe Banana culture medium, *Carbohydr Polym.* Jul. 240 (2020), 116341, <https://doi.org/10.1016/j.carbpol.2020.116341>.
- [29] C. Castro, R. Zuluaga, J.-L. Putaux, G. Caro, I. Mondragon, P. Gañán, Structural characterization of bacterial cellulose produced by *Gluconacetobacter swingsii* sp. from Colombian agroindustrial wastes, *Carbohydr. Polym.* 84 (2011) 96–102, <https://doi.org/10.1016/j.carbpol.2010.10.072>.
- [30] C. Castro, I. Cleenwerck, J. Trček, R. Zuluaga, P. De Vos, G. Caro, et al., *Gluconacetobacter medellinensis* sp. nov., cellulose- and non-cellulose-producing acetic acid bacteria isolated from vinegar, *Int. J. Syst. Evol. Microbiol.* 63 (2013) 1119–1125, <https://doi.org/10.1099/ijs.0.043414-0>.
- [31] M. Osorio, J. Velásquez-Cock, L.M. Restrepo, R. Zuluaga, P. Gañán, O.J. Rojas, et al., Bioactive 3D-shaped wound dressings synthesized from bacterial cellulose: effect on cell adhesion of polyvinyl alcohol integrated in situ, *Int J Polym Sci* 2017 (2017) 1–10.
- [32] C. Molina-Ramírez, M. Castro, M. Osorio, M. Torres-Taborda, B. Gómez, R. Zuluaga, et al., Effect of different carbon sources on bacterial nanocellulose production and structure using the low pH resistant strain *Komagataeibacter medellinensis*, *Materials* 10 (2017) 639, <https://doi.org/10.3390/ma10060639>.
- [33] J. Wang, X. Guo, Adsorption isotherm models: classification, physical meaning, application and solving method, *Chemosphere* 258 (2020), 127279, <https://doi.org/10.1016/j.chemosphere.2020.127279>.
- [34] Velandia Castellanos, Varela González, Aplicaciones Y generalidades de un espectrofotómetro UV-vis Uv-1800 de Shimadzu, 2018.
- [35] R. Saadi, Z. Saadi, R. Fazaeli, N.E. Fard, Monolayer and multilayer adsorption isotherm models for sorption from aqueous media, *Kor. J. Chem. Eng.* 32 (2015) 787–799, <https://doi.org/10.1007/s11814-015-0053-7>.
- [36] A. Ebadi, J.S. Soltan Mohammadzadeh, A. Khudiev, What is the correct form of BET isotherm for modeling liquid phase adsorption? *Adsorption* 15 (2009) 65–73, <https://doi.org/10.1007/s10450-009-9151-3>.
- [37] G.W. Kajjumba, S. Emik, A. Öngen, H.K. Özcan, S. Aydin, Modelling of adsorption kinetic processes—errors, theory and application, in: *Adv Sorption Process Appl.* 2019, pp. 1–19, <https://doi.org/10.5772/intechopen.80495>.
- [38] K.D. de Yao, T. Peng, H.B. Feng, Y.Y. He, Swelling kinetics and release characteristic of crosslinked chitosan: polyether polymer network (semi-IPN) hydrogels, *J. Polym. Sci. Polym. Chem.* 32 (1994) 1213–1223, <https://doi.org/10.1002/pola.1994.080320702>.
- [39] D.R. Bhumkar, V.B. Pokharkar, Studies on effect of pH on cross-linking of chitosan with sodium tripolyphosphate: a technical note, *AAPS PharmSciTech* 7 (2006) E50, <https://doi.org/10.1208/pt070250>.
- [40] G. Sandri, M.C. Bonferoni, F. Ferrari, M. Mori, C. Caramella, C. Caramella, The role of chitosan as a mucoadhesive agent in mucosal drug delivery, *J. Drug Deliv. Sci. Technol.* 22 (2012) 275–284, [https://doi.org/10.1016/S1773-2247\(12\)50046-8](https://doi.org/10.1016/S1773-2247(12)50046-8).
- [41] C. Pan, J. Qian, C. Zhao, H. Yang, X. Zhao, H. Guo, Study on the relationship between crosslinking degree and properties of TPP crosslinked chitosan nanoparticles, *Carbohydr. Polym.* 241 (2020), 116349, <https://doi.org/10.1016/j.carbpol.2020.116349>.
- [42] B. Li, C.L. Shan, Q. Zhou, Y. Fang, Y.L. Wang, F. Xu, et al., Synthesis, characterization, and antibacterial activity of cross-linked chitosan-glutaraldehyde, *Mar. Drugs* 11 (2013) 1534–1552, <https://doi.org/10.3390/md11051534>.
- [43] I. Corazzari, R. Nisticò, F. Turci, M.G. Faga, F. Franzoso, S. Tabasso, et al., Advanced physico-chemical characterization of chitosan by means of TGA coupled online with FTIR and GCMS: thermal degradation and water adsorption capacity, *Polym. Degrad. Stabil.* 112 (2015) 1–9, <https://doi.org/10.1016/j.polyimdegradstab.2014.12.006>.
- [44] C.H. Giles, T.H. MacEwan, S.N. Nakhwa, D. Smith, Studies in adsorption. Part XI.* A System of Classification of Solution Adsorption Isotherms, and its Use in Diagnosis of Adsorption Mechanisms and in Measurement of Specific Surface Areas of Solids. By 846 (1960) 3973–3993, <https://doi.org/10.1039/JR960003973>.
- [45] H.H. Hartgrink, E.P. Jansen, N.C. van Grieken, C.J. van de Velde, Gastric cancer, *Lancet* 374 (2009) 477–490, [https://doi.org/10.1016/S0140-6736\(09\)60617-6](https://doi.org/10.1016/S0140-6736(09)60617-6).
- [46] Y. Wang, J. Lu, B. Jiang, J. Guo, The roles of curcumin in regulating the tumor immunosuppressive microenvironment, *Oncol. Lett.* 19 (2020) 3059–3070, <https://doi.org/10.3892/ol.2020.11437>.
- [47] N. Angelina, I.R. Suhito, C.H. Kim, G.P. Hong, C.G. Park, S.H. Bhang, et al., A fibronectin-coated gold nanostructure composite for electrochemical detection of effects of curcumin-carrying nanoliposomes on human stomach cancer cells, *Analyst* 145 (2020) 675–684, <https://doi.org/10.1039/c9an01553a>.
- [48] M.S. Ali, V. Pandit, M. Jain, K.L. Dhar, Mucoadhesive microparticulate drug delivery system of curcumin against *Helicobacter pylori* infection: design, development and optimization, *J. Adv. Pharm. Technol. Research* (JAPTR) 5 (2014) 48–56.
- [49] G. Ruiz-Pulido, D. Quintanar-Guerrero, L.E. Serrano-Mora, D.I. Medina, Triborheological analysis of reconstituted gastrointestinal mucus/chitosan:TPP nanoparticles system to study mucoadhesion phenomenon under different pH conditions, *Polymers* 14 (2022) 4978, <https://doi.org/10.3390/polym14224978>.
- [50] T.M. M Ways, W.M. Lau, V.V. Khutoryanskiy, Chitosan and its derivatives for application in mucoadhesive drug delivery systems, *Polymers* 10 (2018) 267, <https://doi.org/10.3390/polym10030267>.
- [51] FDA, U.S food & drug administration, GRAS notice inventory 3 (2021).